

ADDIS ABABA UNIVERSITY
SCHOOL OF GRADUATE STUDIES
DEPARTMENT OF CHEMISTRY



**Electrochemical Detection of Methyl Parathion using
poly-(4-amino-3-hydroxynaphthalene-1-sulphonic acid)
Modified Glassy Carbon Electrode**

**A Graduate Project Submitted to School of Graduate Studies Addis
Ababa University in Partial Fulfillment of the Requirements for the
Degree of Master of Science in Chemistry**

**BY
Yoseph Bereket**

**Advisor
Shimelis Admasie (PhD)**

July 2009

Acknowledgment

I would like to thank God for enabling me accomplish this project.

My advisor, Dr. Shimelis Admassie, is the one to whom I would like to address my heart felt thanks. Without him it would be very hard for me to reach where I am now. He was beside me from the beginning with his continuous advise, support, inspiration and friendly approach.

Last but not least, I would like to thank my family and friends for lending me their comfortable shoulder where I lean on all the way. And everyone who was there when I needed any kind of support. Thank you all.

List of Figures

Figures	Pages
Fig. 1. Polyacetylene, A commonly known polymer.....	4
Fig. 2. Illustration of the energies involved in a molecular ionization process. E_{IP-v} is the vertical ionization energy, E_{rel} the relaxation energy gained in the ionized state, E_{dis} , the distortion energy to be paid in the ground state in order that the molecule adopts the equilibrium geometry of the ionized state, and E_{IP-d} , the ionization energy of the distorted molecule.....	6
Fig. 3. Schematic illustration of the one-electron energy levels for an organic molecule in its ground-state electronic configuration adopting: (a) the equilibrium geometry of the ground state; (b) the equilibrium geometry of the first ionized state.....	6
Fig. 4. Illustration of the band structure of a polymeric chain in the case of (a) a vertical ionization process and (b) the formation of a polaron. The chemical potential, or Fermi level, is taken as reference level.....	8
Fig. 5. Band structure of a polymer chain containing: (a) two polarons; (b) one bipolaron.....	8
Fig. 6. Total energy curve for an infinite trans-polyacetylene chain as a function of the degree of bond length alternation Δr	10
Fig. 7. Illustration of the formation of two charged solitons on a chain of trans-polyacetylene...	11
Fig. 8. Top: schematic illustration of the geometric structure of a neutral soliton on a trans-polyacetylene chain. Bottom: band structure for a trans-polyacetylene chain containing (a) a neutral soliton, (b) a positively charged soliton, and (c) a negatively charged soliton.....	12
Fig. 9. Three-electrode setup:(1)working electrode; (2)auxiliary electrode; (3)reference electrode	
Fig. 10. Linear sweep voltammetry waveform.....	15
Fig. 11. cyclic voltammetry waveform (A) and Typical cyclic voltammogram (B).....	16
Fig. 12. Differential pulse waveform (A) and Square wave waveform (B).....	22
Fig. 13. (A) continuous cyclic voltammogram of AHNSA in 0.1M HNO ₃ ; (B) the 26 th cyclic voltammogram of AHNSA in 0.1MHNO ₃ ; scan rate: 100mV/s, switching potentials: +2000mV and -800mV.....	32

Fig. 14. cyclic voltammogram at poly-AHNSA/GCE modified electrode in pH 5 acetate buffer solution; scan rate: 100mV/s, switching potentials: +800mV and -800mV.....	33
Fig. 15. Continuous CV response of 8 μ M MPT at the poly-AHNSA modified GCE in pH5 acetate buffer. Scan rate: 100mV/s; switching potentials: +800mV and -1200mV.....	34
Fig. 16. Cyclic voltammograms of 8 μ M MPT at bare GCE (a) and poly-AHNSA/GCE. Scan rate: 100mV/s; switching potentials: +800mV and -1200mV.....	36
Fig. 17. Square wave (a), differential pulse (b) voltammetric response of 10 μ M MPT at the poly-AHNSA/GCE in pH acetate buffer. Scan rate: 100mV/s; $P_p = -0.4V$; $t_p = 50$ s.....	37
Fig. 18. Effect of P_p on square wave voltammetric response for 8 μ M MPT in pH 5 acetate buffer at poly-AHNSA/GCE. $t_p = 50$ s; SW amplitude:25mV; frequency: 15mV; step : 4mV.....	38
Fig. 19. Effect of t_p on square wave voltammetric response for 8 μ M MPT in pH 5 acetate buffer at poly-AHNSA/GCE. $P_p = -0.4$ s; SW amplitude:25mV; frequency: 15mV; step : 4mV.....	39
Fig. 20. pH dependence of peak current on SW voltammetric response for 8 μ M MPT at the poly-AHNSA/GCE. $P_p = -0.4V$; $t_p = 50$ s; SW amplitude:25mV; frequency: 15mV; step:4mV.....	40
Fig. 21. (A) Square wave voltammograms of increasing concentration of MPT at poly-AHNSA/GCE in pH 5 acetate buffer. (a) blank solution; (b) $0.2 \times 10^{-6}M$; (c) $0.4 \times 10^{-6}M$; (d) $0.8 \times 10^{-6}M$; (e) $1.2 \times 10^{-6}M$; (f) $1.6 \times 10^{-6}M$. $P_p = -0.4V$; $t_p = 50$ s; SW amplitude:25mV; frequency: 15mV; step : 4mV.....	41
Fig. 22. A plot of peak current Vs MPT concentration. $P_p = -0.4V$; $t_p = 50$ s; SW amplitude:25mV; frequency: 15mV; step : 4mV.....	42

Contents

	Pages
Acknowledgment	i
List of Figures.....	ii
Contents	iv
Abstract	vi
1. Introduction	1
2. Theoretical Background	3
2.1. Conducting polymers	3
2.1.1. Conduction mechanism	4
2.2. Voltammetric Techniques	12
2.2.1. LSV and Cyclic Voltammetry	14
2.2.2. Pulsed Voltammetric Techniques	21
2.3. Pesticides	24
2.3.1. Need for Pesticides Analysis	24
2.3.2. Organophosphorous pesticides	25
3. Literature Review	27
4. Objective of the Study	29
5. Experimental	30
5.1. Apparatus	30
5.2. Reagents	30
5.3. Procedures	30

5.3.1. Preparation of Poly-AHNSA/GCE	30
5.3.2. Measurement Procedures	31
6. Discussion	32
6.1. Electropolymerization of AHNSA	32
6.2. Electrochemical Behavior of Methyl Parathion	34
6.3. Effect of poly-AHNSA on MPT Detection	36
6.4. Optimization of Parameters for MPT Detection	37
6.4.1. Effect of Accumulation Potential (P_p)	38
6.4.2. Effect of Accumulation Time (t_p)	39
6.4.3. Effect of Solution pH	40
6.5. Analytical characterization	41
7. Conclusion	43
References	44

Abstract

A glassy carbon electrode (GCE) was modified with electropolymerization of 4-Amino-3-Hydroxynaphthalene-1-Sulphonic acid (AHNSA) in 0.1M HNO₃ using cyclic voltammetry. The modified electrode showed an excellent electrocatalytic effect on the redox property of Methyl Parathion. The bare glassy carbon electrode could barely sense the 8μM concentration solution of MPT. The modified electrode showed all the expected peaks from the MPT with high sensitivity. After the optimization of Different parameters, analytical characterization of MPT was made. The peak current increases linearly with the range of concentration of MPT used in the analysis (0.2μM-1.6μM). The detection limit was 6.3 x 10⁻⁸M by square wave voltammetry. The modified electrode has successfully been applied for the detection of MPT.

Key words: Conducting Polymers, Electropolymerization, Organophosphorous Pesticides, AHNSA, Methyl Parathion, Voltammetric technique

1. Introduction

Since the introduction of conducting polymers many improvements are made in the electrochemical sensing aspects. Their conjugated π -electrons are responsible for their electronic property. They are electrically conductive, have low energy optical transitions, low ionization potential and high electron affinity [1].

Many applications of conducting polymers including biosensing devices and analytical chemistry have been reported. One of their applications, of our interest, is in the detection of pesticides.

Pesticides are any substances used for destroying pests. They have different properties and are used for different kinds of pests. For instance, organophosphorous pesticides (OPPs) tend to inhibit the acetylcholine esterase of the organism, which blocks the nervous transmission and cause death by respiratory depression. [2]

Despite to their contribution for the modern life style of human beings, their environmental pollution has been a headache for many scientists. Thus, methods are continually sought for an effective detection and determination of pesticide levels in the environment.

Methyl Parathion (MPT) is one of the environmentally hazardous pesticides that effective methods of detecting and controlling are sought for. MPT is an organophosphorous pesticide introduced onto the agricultural market in the early 1950s. This insecticide is widely used to control chewing and sucking insects in a wide range of crops, including cereals, fruits, vegetables, ornamentals, cotton and field crops. Like the other organophosphorous pesticides it inhibits the cholinesterase enzyme. The toxic effect of MPT in animals occurs by inhibition of

acetyl cholinesterase. It is a very toxic compound which can lead to the pollution of the environment and is classified as extremely hazardous pesticide by the World Health Organization (WHO) and can constitute public health concerns. [3]

In this project, a glassy carbon electrode is modified with a conducting polymer (poly-AHNSA) for an electrochemical detection of methyl parathion.

2. Theoretical Background

2.1. Conducting polymers

Conductive polymers are a sub-group of a larger, older group of organic and inorganic electrical conductors. In fact, as early as 1862 H. Letheby of the College of London Hospital, by anodic oxidation of aniline in sulphuric acid, obtained a partly conductive material which was probably polyaniline. In the early 1970s, it was found that the inorganic explosive polymer, poly(sulphur nitride) (SN)_x, was superconductive at extremely low temperatures ($T_c=0.26$ K). Many conductive organic compounds were also known, such as those discovered by K. Bechgaard (Copenhagen) together with D. Jerome (Paris) and famous for being superconductive at rather “high” temperatures (T_c around 10 K). They are salts of inorganic acceptors and organic donors consisting of large, cyclically conjugated π -electron systems that form coin-pile stacks in the solid state. However, polyacetylene was the conductive polymer that actually launched this new field of research [4].

It was discovered that polyacetylene, which has an intrinsic conductivity much lower than $10^{-5}(\Omega\cdot\text{cm})^{-1}$, could be made highly conducting $\sim 10^{-3}(\Omega\cdot\text{cm})^{-1}$, by exposing it to oxidizing or reducing agent. This process is often referred to as "doping" by analogy with the doping of inorganic semiconductors. This is a rather misleading analogy, however, and the process is best viewed as a redox reaction. The insulating neutral polymer is converted into anionic complex consisting of a polymeric cation (or anion) and a counter ion which is the reduced form of the oxidizing agent (or the oxidized form of the reducing agent). In solid-state physics terminology, the use of an oxidizing agent corresponds to p-type doping and that of a reducing agent to n-type doping. An important criterion in selecting potentially conducting polymers is therefore the ease with which the system can be oxidized or reduced. This accounts in part for the choice of π -

bonded unsaturated polymers which, like polyacetylene, have small ionization potentials and/or large electron affinities. Electrons of π character can be relatively easily removed or added to form a polymeric ion without much disruption of the σ -bonds which are primarily responsible for holding the polymer together [5].

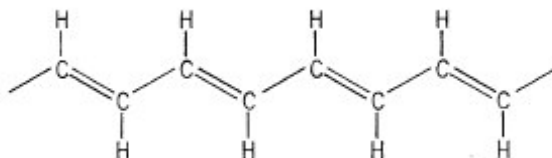


Fig. 1. Polyacetylene, A commonly known polymer.

Conducting polymers contain π -electron backbone responsible for their unusual electronic properties such as electrical conductivity, low energy optical transitions, low ionization potential and high electron affinity. This extended π -conjugated system of the conducting polymers have single and double bonds alternating along the polymer chain. The higher values of the electrical conductivity obtained in such organic polymers have led to the name 'synthetic metals'. Many applications of conducting polymers including analytical chemistry and bio-sensing devices have been reviewed by various researchers. They have widened the possibility of modification of surface of conventional electrodes providing new and interesting properties. They also create new technological possibilities in design of chemical and biochemical sensors [1].

2.1.1. Conduction mechanism

A polymer is transformed into a conductor by doping it with either an electron donator or an electron acceptor. This is reminiscent of doping of silicon based semiconductors where silicon is

doped with either arsenic or boron. However, while the doping of silicon produces a donor energy level close to the conduction band or an acceptor level close to the valence band, this is not the case with conducting polymers. The evidence for this is that the resulting polymers do not have a high enough concentration of free spins (the conductivity does not seem to be associated with unpaired electrons but rather with spinless charge carriers).

The mechanism of conduction in such polymers is very complex since such a material exhibits conductivity across a range of about fifteen orders of magnitude and many involve different mechanisms within different regimes. Conducting polymers show enhanced electrical conductivity by several orders of magnitude of doping. The concept of solitons, polarons and bipolarons has been used to explain the electronic phenomena in these systems [1, 6].

In organic molecules, it is usually the case that the equilibrium geometry in the ionized state is different from that in the ground state. The energies involved in the ionization process of a molecule are schematically depicted in Figure 2. A vertical ionization process costs an energy E_{IP-v} . If a geometry relaxation then takes place in the ionized state, we gain back relaxation energy E_{rel} . Conceptually, going from the ground state to the relaxed ionized state can also be thought of in the following way. The geometry of the molecule is first distorted in the ground state in such a way that the molecule adopts the equilibrium geometry of the ionized state. This costs a distortion (elastic) energy E_{dis} (Figure 2). If we consider the one-electron energy levels of the molecule, this distortion leads to an upward shift $\Delta\epsilon$ of the highest occupied molecular orbital (HOMO) and a downward shift of the lowest unoccupied molecular orbital (LUMO), as illustrated in Figure 3. If we then proceed to the ionization of the distorted molecule, it requires an energy E_{IP-d} .

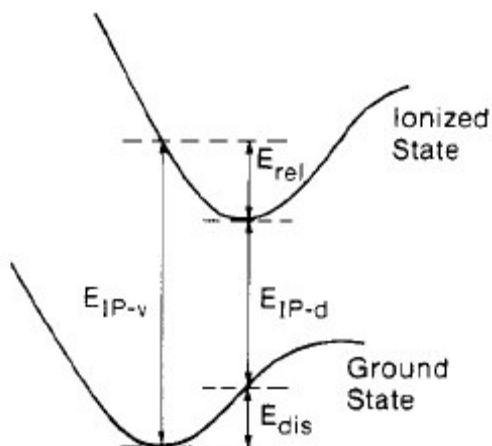


Fig. 2. Illustration of the energies involved in a molecular ionization process. E_{IP-v} is the vertical ionization energy, E_{rel} the relaxation energy gained in the ionized state, E_{dis} , the distortion energy to be paid in the ground state in order that the molecule adopts the equilibrium geometry of the ionized state, and E_{IP-d} , the ionization energy of the distorted molecule.

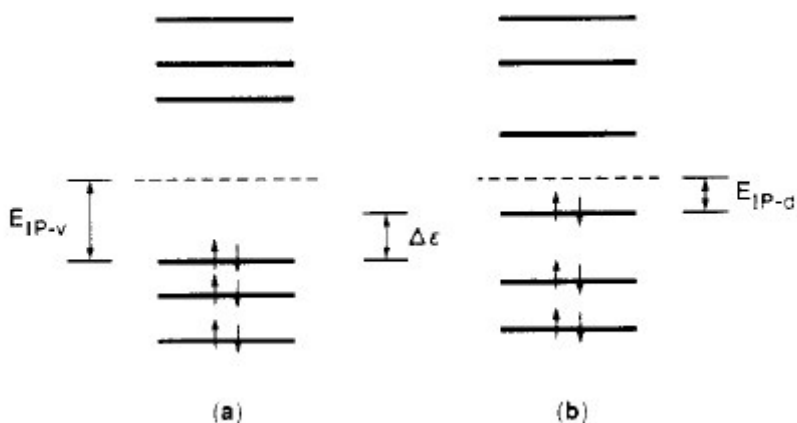


Fig. 3. Schematic illustration of the one-electron energy levels for an organic molecule in its ground-state electronic configuration adopting: (a) the equilibrium geometry of the ground state; (b) the equilibrium geometry of the first ionized state.

From Figure 2, it is clear that it is energetically favorable to have a geometry relaxation in the ionized state when the quantity $E_{IP-v} - E_{IP-d}$ (which actually corresponds to $\Delta\epsilon$) is larger than the distortion energy E_{dis} ; or, in other words, when the reduction $\Delta\epsilon$ in ionization energy upon distortion is larger than the energy E_{dis} required to make that distortion.

In a polymer, or any solid, a vertical ionization process E_{IP-v} results in creating a hole on top of the valence band;(Figure 4a). In this case, three remarks can be made. First, by the very definition of the process, no geometry relaxation (lattice distortion) takes place on the chain. Second, the positive charge on the chain is delocalized over the whole polymer chain. Third, the presence of a hole (unfilled level) on top of the VB leads to the appearance of a metallic character. This situation corresponds to the initial assumption made about the conduction mechanism in doped organic polymers.

However, in an organic polymer chain, it can be energetically favorable to localize the charge that appears on the chain and to have, around the charge, a local distortion (relaxation) of the lattice. This process causes the presence of localized electronic states in the gap due to a local upward shift $\Delta\epsilon$ of the HOMO and downward shift of the LUMO (Figure 4b). Considering the case of oxidation, i.e., the removal of an electron from the chain, we lower the ionization energy by an amount $\Delta\epsilon$. If $\Delta\epsilon$ is larger than the energy E_{dis} necessary to distort the lattice locally around the charge, this charge localization process is favorable relative to the band process. We then obtain the formation of what condensed-matter physicists call a polaron.

The quantity $\Delta\epsilon - E_{dis}$ ($= E_{rel}$) corresponds to the polaron binding energy. The polaron binding energy is of the order of 0.05 eV in PA, 0.03 eV in PPP and 0.12 eV in PPy. It must be stressed that in the case of polaron formation, the VB remains full and the CB empty. There is no appearance of metallic character since the half-occupied level is localized in the gap (Figure 4b).

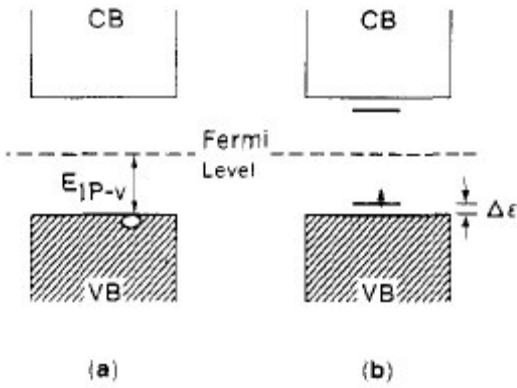


Fig. 4. Illustration of the band structure of a polymeric chain in the case of (a) a vertical ionization process and (b) the formation of a polaron. The chemical potential, or Fermi level, is taken as reference level.

When a second electron is removed from the polymer chain, there will be a bipolaron formation. A bipolaron is defined as a pair of like charges (here a dication) associated with a strong local lattice distortion. The bipolaron can be thought of as analogous to the Cooper pair in the BCS theory of superconductivity, which consists of two electrons coupled through a lattice vibration. The formation of a bipolaron implies that the energy gained by the interaction with the lattice is larger than the Coulomb repulsion between the two charges of same sign confined in the same location.

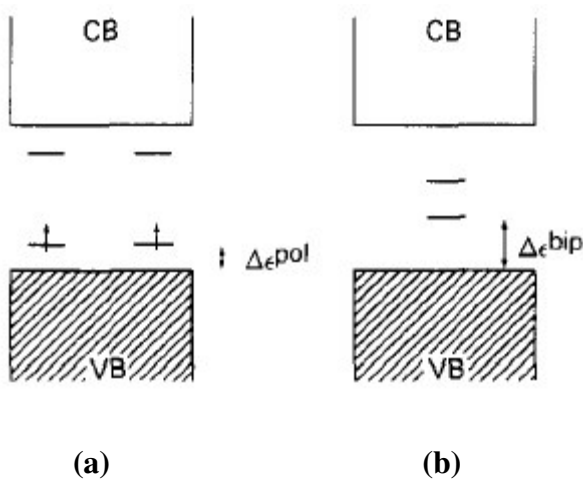


Fig. 5. Band structure of a polymer chain containing: (a) two polarons; (b) one bipolaron.

The electronic band structure corresponding to the presence of two polarons and that of one bipolaron is depicted in Figure 5. Since the lattice relaxation around two charges is stronger than around only one charge, E_{dis} for the bipolaron is larger than E_{dis} for the polaron and the electronic states appearing in the gap for a bipolaron are further away from the band edges than for a polaron.

In case of p- (n-) type doping, the bipolaron levels in the gap are empty (fully occupied). The bipolarons are thus spinless. The presence of bipolarons on polymer chains result in the possibility of two optical transitions below the band gap transition: for p-type doping, from the VB to the lower bipolaron level and from the VB to the upper bipolaron level. The oscillator strength for the lowest energy optical bipolaron transition has been calculated to be much larger than for the highest energy one. In the case of polarons, a third absorption is possible below the gap, corresponding to an optical transition between the two polaron levels (Figure 5a).

Conjugated polymers with a degenerate ground state have a slightly different mechanism. trans-Polyacetylene is unique so far among conducting polymers because it possesses a degenerate ground state, i.e., two geometric structures corresponding exactly to the same total energy (Figure 6). The two structures differ from one another by the exchange of the carbon-carbon single and double bonds.

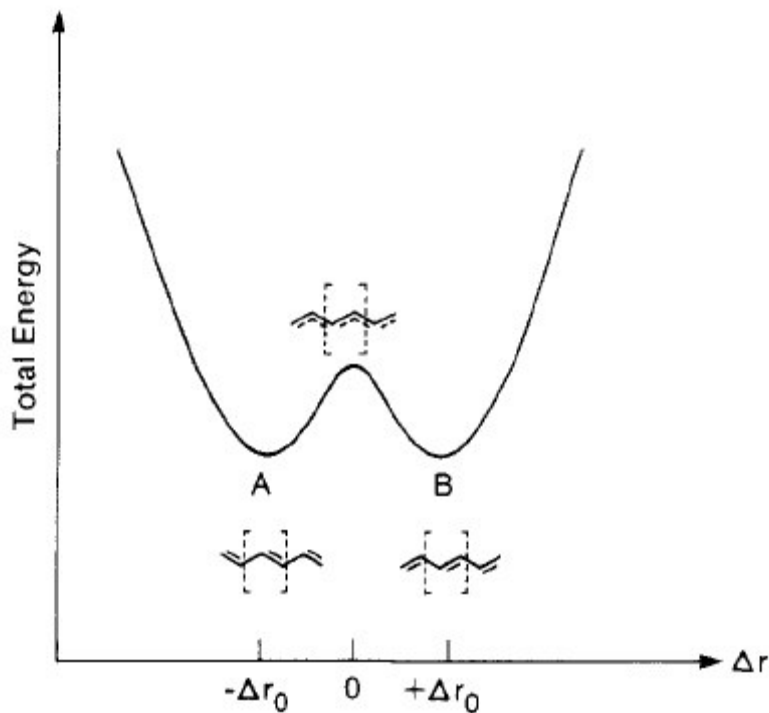


Fig. 6. Total energy curve for an infinite trans-polyacetylene chain as a function of the degree of bond length alternation Δr .

As a result of the degeneracy, the two charges forming a would-be bipolaron in trans-PA can readily separate (Figure 7). This process is favorable because there is no increase in distortion energy when the two charges separate, since the geometric structure that appears between the two charges has the same energy as the geometric structure on the other sides of the charges. From Figures 6 and 7, it is apparent that an isolated charge on a trans-PA chain constitutes a boundary between a segment of the chain adopting the geometric structure corresponding to one of the potential wells and a segment adopting the structure corresponding to the other well. Such a charge associated with a boundary or domain wall is called a soliton.

A soliton can be viewed as an excitation of the system that leads from one potential well to another well of the same energy (Figure 6). A neutral soliton occurs in pristine trans-PA when a chain contains an odd number of conjugated carbons, in which case there remains an unpaired π -electron, a radical, which corresponds to a soliton (Figure 8). In a long chain, the spin density in a neutral soliton (or charge density in a charged soliton) is not localized on one carbon but spread over several carbons, which gives the soliton a width. Starting from one side of the soliton, the double bonds become gradually longer and the single bonds shorter, so that arriving at the other side, the alternation has completely reversed. This implies that the bond lengths do equalize in the middle of a soliton. The presence of a soliton leads to the appearance of a localized electronic level at mid-gap, which is half-occupied in the case of a neutral soliton and empty (doubly occupied) in the case of a positively (negatively) charged soliton. Compared to a polaron, the soliton has unusual spin-charge relationships: since a neutral soliton is a radical, it has a spin $1/2$ whereas a charged soliton is spinless [5].

2.2. Voltammetric Techniques

Voltammetry is a category of electroanalytical methods used in analytical chemistry and various industrial processes. It comprises a group of electrochemical methods in which information about the analyte is derived from the measurement of current as a function of applied potential, the measurements being obtained under conditions that encourage polarization of an indicator, or working electrode. [7]

Voltammetry experiments investigate the half cell reactivity of an analyte. Most experiments control the potential (volts) of an electrode in contact with the analyte while measuring the resulting current (amperes).

To conduct such an experiment requires at least two electrodes. The working electrode, which makes contact with the analyte, must apply the desired potential in a controlled way and facilitate

the transfer of electrons to and from the analyte. A second electrode acts as the other half of the cell. This second electrode must have a known potential with which to gauge the potential of the working electrode, furthermore it must balance the electrons added or removed by the working electrode. While this is a viable setup, it has a number of shortcomings. Most significantly, it is extremely difficult for an electrode to maintain a constant potential while passing current to counter redox events at the working electrode.

To solve this problem, the role of supplying electrons and referencing potential has been divided between two separate electrodes. The reference electrode is a half cell with a known reduction potential. Its only role is to act as reference in measuring and controlling the working electrodes potential and at no point does it pass any current. The auxiliary electrode passes all the current needed to balance the current observed at the working electrode. To achieve this current, the auxiliary will often swing to extreme potentials at the edges of the solvent window, where it oxidizes or reduces the solvent or supporting electrolyte. These electrodes, the working, reference, and auxiliary make up the modern three electrode system.

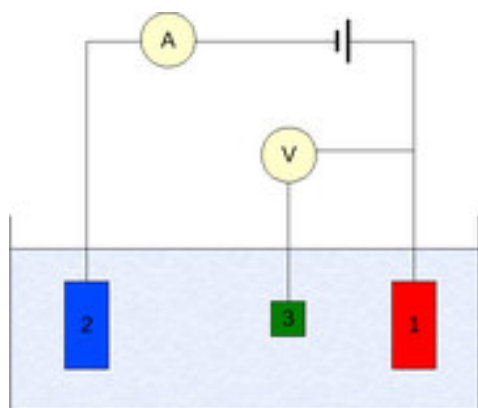


Fig. 9. Three-electrode setup:(1)working electrode; (2)auxiliary electrode; (3)reference electrode

There are many systems which have more electrodes, but their design principles are generally the same as the three electrode system. For example, the rotating ring-disk electrode has two distinct and separate working electrodes, a disk and a ring, which can be used to scan or hold potentials

independently of each other. Both of these electrodes are balanced by a single reference and auxiliary combination for an over all four electrode design. More complicated experiments may add working electrodes as required and at times reference or auxiliary electrodes.

In practice it can be very important to have a working electrode with known dimensions and surface characteristics. As a result, it is common to clean and polish working electrodes regularly. The auxiliary electrode can be almost anything as long as it doesn't react with the bulk of the analyte solution and conducts well. The reference is the most complex of the three electrodes, there are a variety of standards used and its worth investigating elsewhere. For non-aqueous work, IUPAC recommends the use of the ferrocene/ferrocenium couple as an internal standard. In most voltammetry experiments a bulk electrolyte (also known as supporting electrolyte) is used to minimize solution resistance. It can be possible to run an experiment without a bulk electrolyte but the added resistance greatly reduces accuracy of the results. In the case of room temperature ionic liquids the solvent can act as the electrolyte.

There are different types of voltammetry depending on potential wave supplied for the analysis. Among these Linear sweep voltammetry, Cyclic voltammetry, Square wave voltammetry, and Differential wave voltammetry are most commonly used in different electroanalytical experiments.

2.2.1. Linear Sweep and Cyclic Voltammetry

Linear sweep voltammetry is a voltammetric method where the current at a working electrode is measured while the potential between the working electrode and a reference electrode is swept linearly in time. Oxidation or reduction of species is registered as a peak or trough in the current signal at the potential at which the species begins to be oxidized or reduced.

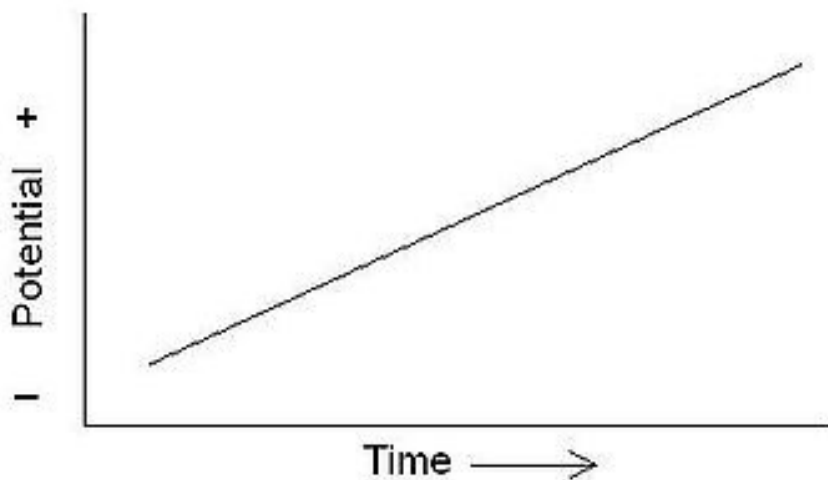


Fig. 10. Linear sweep voltammetry waveform

Cyclic voltammetry or CV is a type of potentiodynamic electrochemical measurement. In a cyclic voltammetry experiment the working electrode potential is ramped linearly versus time like linear sweep voltammetry. In this method the reversal experiment of linear scan voltammetry is carried out by switching the direction of the scan at a certain time (or a switching potential) [8]. This reversal can happen multiple times during a single experiment. The current at the working electrode is plotted versus the applied voltage to give the cyclic voltammogram trace. Cyclic voltammetry is generally used to study the electrochemical properties of an analyte in solution.

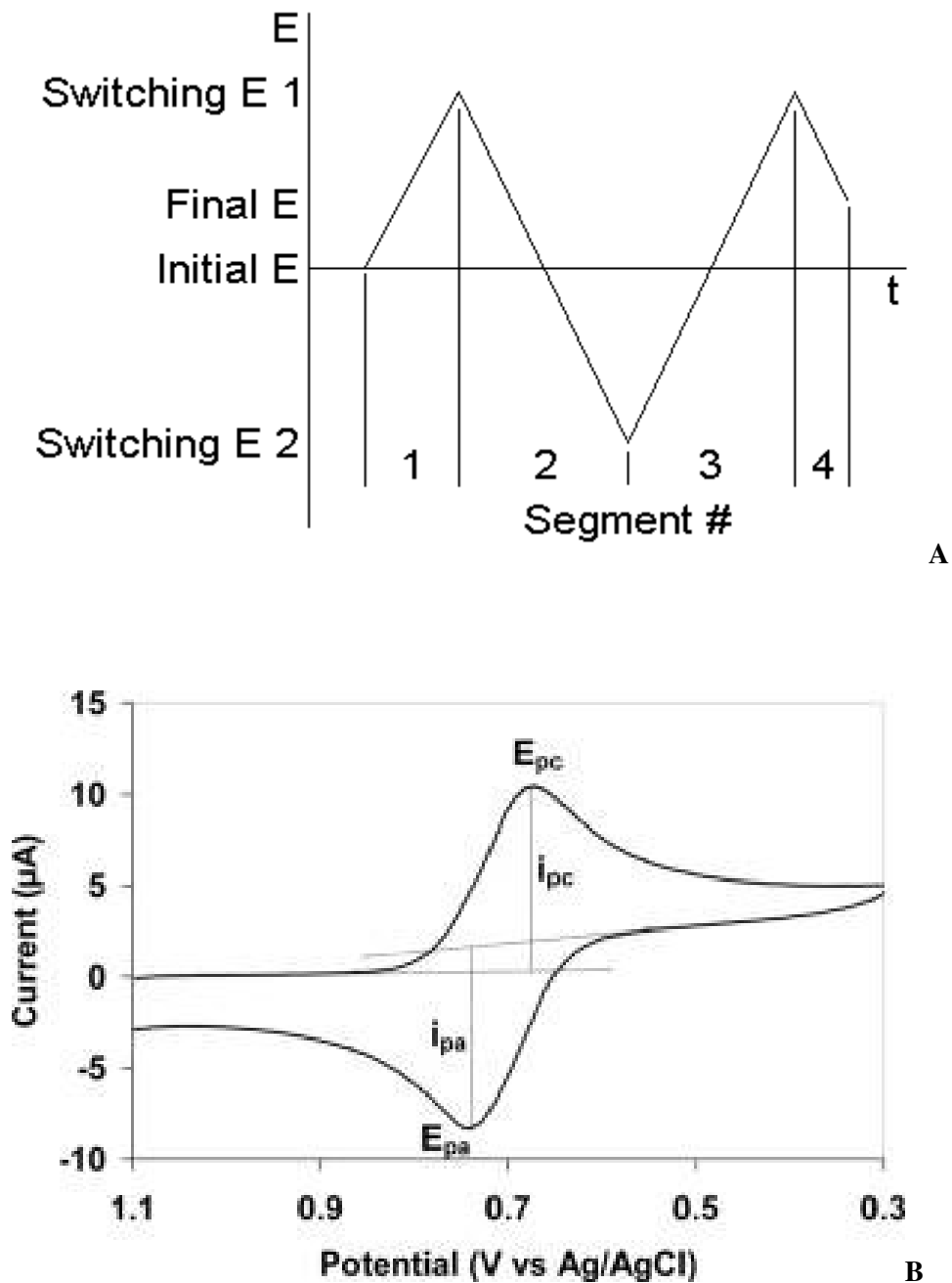


Fig. 11. cyclic voltammetry waveform (A) and Typical cyclic voltammogram (B)

In cyclic voltammetry, the electrode potential ramps linearly versus time as shown. This ramping is known as the experiment's scan rate (V/s). The potential is measured between the reference electrode and the working electrode and the current is measured between the working electrode

and the counter electrode. This data is then plotted as current (i) vs. potential (E). As the waveform shows, the forward scan produces a current peak for any analytes that can be reduced (or oxidized depending on the initial scan direction) through the range of the potential scanned. The current will increase as the potential reaches the reduction potential of the analyte, but then falls off as the concentration of the analyte is depleted close to the electrode surface. If the redox couple is reversible then when the applied potential is reversed, it will reach the potential that will reoxidize the product formed in the first reduction reaction, and produce a current of reverse polarity from the forward scan. This oxidation peak will usually have a similar shape to the reduction peak. As a result, information about the redox potential and electrochemical reaction rates of the compounds are obtained.

For instance if the electronic transfer at the surface is fast and the current is limited by the diffusion of species to the electrode surface, then the current peak will be proportional to the square root of the scan rate. This relationship is described by the Cottrell equation.

The utility of cyclic voltammetry is highly dependent on the analyte being studied. The analyte has to be redox active within the experimental potential window. It is also highly desirable for the analyte to display a reversible wave. A reversible wave is when an analyte is reduced or oxidized on a forward scan and is then reoxidized or rereduced in a predictable way on the return scan as shown in the previous figure.

Even reversible couples contain polarization overpotential and this display a hysteresis between absolute potential between the reduction (E_{pc}) and oxidation peak (E_{pa}). This overpotential emerges from a combination of analyte diffusion rates and the intrinsic activation barrier of transferring electrons from an electrode to analyte. A theoretical description of polarization overpotential is in part described by the Butler-Volmer equation and Cottrell equation.

Conveniently in an ideal system the relationships reduces to, $|E_{pc} - E_{pa}| = \frac{57 \text{ mV}}{n}$, for an n electron process [9].

Reversible couples will display a ratio of the peak currents passed at reduction (i_{pc}) and oxidation (i_{pa}) that is near unity ($1 = i_{pa}/i_{pc}$). This ratio can be perturbed for reversible couples in the presence of a following chemical reaction, stripping wave, or nucleation event.

When such reversible peaks are observed thermodynamic information in the form of half cell potential $E^0_{1/2}$ can be determined. When waves are semi-reversible such as when i_{pa}/i_{pc} is less than or greater than 1, it can be possible to determine even more information especially kinetic processes like following chemical reaction.

When waves are non-reversible it is impossible to determine what their thermodynamic $E^0_{1/2}$ is with cyclic voltammetry. This $E^0_{1/2}$ can be determined however it often requires equal quantities of the analyte in both oxidation states. When a wave is non-reversible cyclic voltammetry can not determine if the wave is at its thermodynamic potential or shift to a more extreme potential by some form of overpotential. The couple could be irreversible because of a following chemical process, a common example for transition metals is a shift in the geometry of the coordination sphere. If this is the case, then higher scan rates may show a reversible wave. It is also possible that the wave is irreversible due to a physical process most commonly some form of precipitation. Some speculation can be made in regards to irreversible waves however they are generally outside the scope of cyclic voltammetry.

The method uses a reference electrode, working electrode, and counter electrode which in combination are sometimes referred to as a three-electrode setup. Electrolyte is usually added to

the test solution to ensure sufficient conductivity. The combination of the solvent, electrolyte and specific working electrode material determines the range of the potential.

Electrodes are static and sit in unstirred solutions during cyclic voltammetry. This "still" solution method results in cyclic voltammetry's characteristic diffusion controlled peaks. This method also allows a portion of the analyte to remain after reduction or oxidation where it may display further redox activity. Stirring the solution between cyclic voltammetry traces is important as to supply the electrode surface with fresh analyte for each new experiment. The solubility of an analyte can change drastically with its overall charge. Since cyclic voltammetry usually alters the charge of the analyte it is common for reduced or oxidized analyte to precipitate out onto the electrode. This layering of analyte can insulate the electrode surface, display its own redox activity in subsequent scans, or at the very least alter the electrode surface. For this and other reasons it is often necessary to clean electrodes between scans.

Common materials for working electrodes include glassy carbon, platinum, and gold. These electrodes are generally encased in a rod of inert insulator with a disk exposed at one end. A regular working electrode has a radius within an order of magnitude of 1 mm. Having a controlled surface area with a defined shape is important for interpreting cyclic voltammetry results.

To run cyclic voltammetry experiments at high scan rates a regular working electrode is insufficient. High scan rates create peaks with large currents and increased resistances which result in distortions. Ultramicroelectrodes can be used to minimize the current and resistance.

The counter electrode, also known as the auxiliary or second electrode, can be any material which conducts easily and won't react with the bulk solution. Reactions occurring at the counter electrode surface are unimportant as long as it continues to conduct current well. To maintain the

observed current the counter electrode will often oxidize or reduce the solvent or bulk electrolyte.

In some experiments an electroactive species is fixed to the surface of the electrode, for instance in microparticle voltammetry.

Potentiodynamic techniques also exist that add low-amplitude ac perturbation to a potential ramp and measure variable response in a single frequency (ac voltammetry) or in many frequencies simultaneously (potentiodynamic electrochemical impedance spectroscopy). The response in alternating current is two-dimensional – it is characterised by amplitude and phase. The amplitude and phase depend differently on frequency for constituents of ac response attributed to different processes (charge transfer, diffusion, double layer charging, etc.). Frequency response analysis enables simultaneous monitoring of the various processes that contribute to the potentiodynamic ac response of electrochemical system.

Cyclic voltammetry is not a hydrodynamic technique. In a hydrodynamic technique flow is achieved at the electrode surface by stirring the solution, pumping the solution, or rotating the electrode as is the case with rotating disk electrodes and rotating ring-disk electrodes. These techniques target steady state conditions which appear the same scanned from the positive or the negative, thus limiting them to linear sweep voltammetry.

2.2.2. Pulsed Voltammetric Techniques

Square wave voltammetry (SWV) and differential pulse voltammetry (DPV) are used for both qualitative and quantitative analysis. These methods take advantage of computer timing to

repeatedly sample current signals at two points relative to the time of application of a square wave voltage signal to the electrode. The difference between the two current values is plotted as a function of the applied DC potential. The resultant is peaks rather than voltammetric waves, corresponding to the electroactivity of the species in the electrochemical cell. The major component of this difference current is the faradaic current, which flows due to an oxidation or reduction at the electrode surface. The capacitive or charging current component, due to electrical charging of electrode double layer, is largely eliminated. This increases the signal to noise ratio.

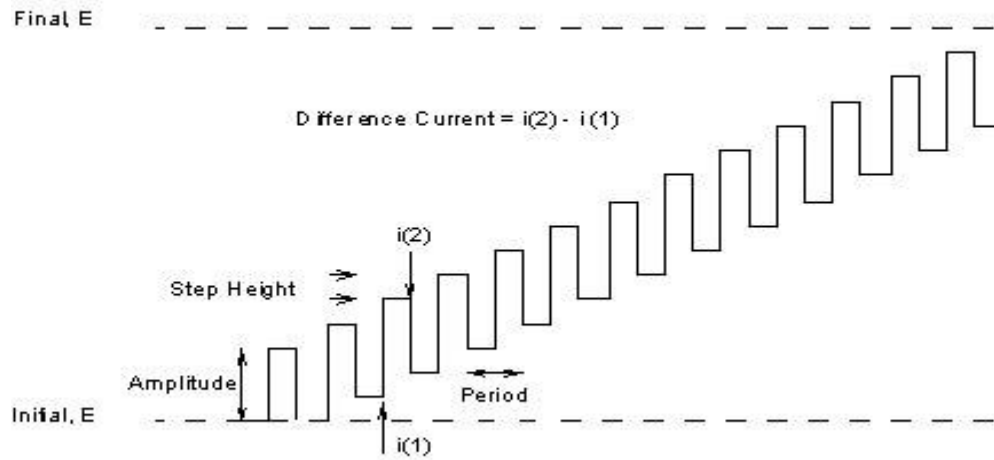
The difference in the two techniques is in the detail of the applied potential pulsed waveform.

Differential Pulse Voltammetry

Two current measurements are made alternatively. The difference in current per pulse (Δi) is recorded as a function of the linearly increasing voltage. A differential curve results that consists of a peak the height of which is directly proportional to concentration. For reversible reaction the peak potential is approximately equal to the standard potential for the half-reaction.

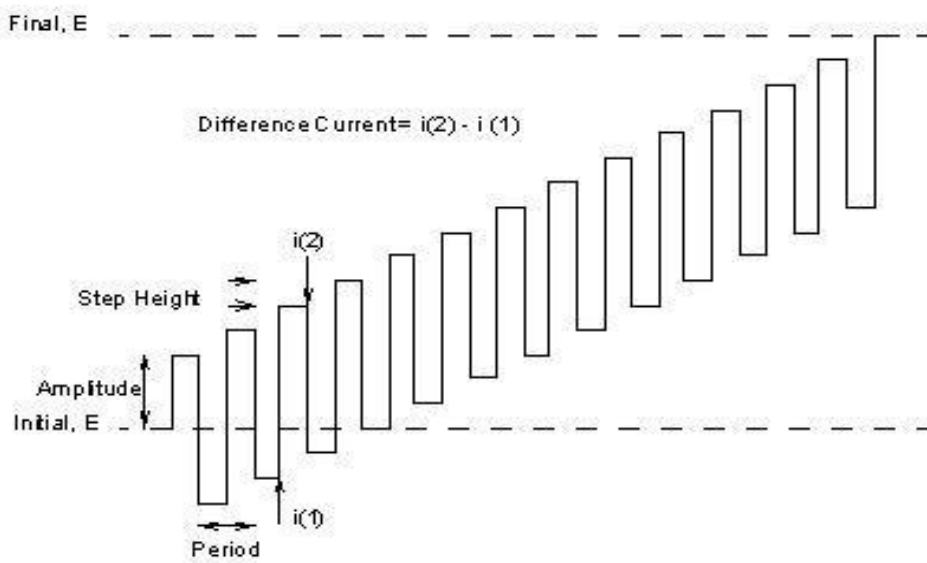
One advantage of the derivative-type polarogram is that individual peak maxima can be observed for substances with half-wave potentials differing by as little as 0.04 to 0.05V. More importantly, differential pulse Voltammetry increases the sensitivity of the voltammetric method significantly. [10]

Differential Pulse Waveform



A

Square Wave Waveform



B

Fig. 12. Differential pulse waveform (A) and Square wave waveform (B)

Square Wave Voltammetry

Square wave is a type of voltammetry that offers the advantage of great speed and high sensitivity. It can be viewed as combining the best aspects of several pulse voltammetric methods, including the background suppression and sensitivity of differential pulse voltammetry, the diagnostic value of normal pulse voltammetry, and the ability to interrogate products directly in much the manner of reverse pulse voltammetry [8].

The excitation signal in SWV consists of a symmetrical square-wave pulse of amplitude E_{sw} superimposed on a staircase wave form of step height ΔE , where the forward pulse of the square wave coincides with the staircase step. The net current, i_{net} , is obtained by taking the difference between the forward and reverse currents ($i_{for} - i_{rev}$) and is centered on the redox potential. The peak height is directly proportional to the concentration of the electroactive species and direct detection limit as low as $10^{-8}M$ is possible. [8, 11]

Square wave voltammetry has several advantages. Among these are its excellent sensitivity and the rejection of background currents. Another is the speed. This speed, coupled with computer control and signal averaging, allows for experiments to be performed repetitively and it increases the signal to noise ratio. The net peak current for the irreversible system is given by:[11]

$$I_p = \text{Constant } \alpha n^2 \Delta E E_{sw} (fD)^{1/2} C$$

Where ΔE is the step potential, f is square wave frequency, E_{sw} is square wave amplitude, α is the transfer coefficient, n is the overall electron transfer, C is the bulk concentration and D is the diffusion coefficient of the electroactive species.

Applications of square-wave Voltammetry include the study of electrode kinetics with regard to preceding, following, or catalytic homogeneous chemical reactions, determination of some species at trace levels, and its use with electrochemical detection in HPLC. [12]

2.3. Pesticides

The term pesticide is used to indicate any substance, preparation or organism used for destroying pests. Insecticides, herbicides, fungicides, nematocides, acaricides, lumbricides, growth regulators, insect repellants, are substances that can be grouped under pesticides [2, 13-16].

According to their chemical nature, a first rough classification distinguishes between organic and inorganic pesticides. Actually, organic chemical pesticides receive virtually all of the regulatory attentions and public concern. The most important classes of pesticides are organochlorines, organophosphorous, carbamates, triazines, phenoxyacids, phenyl and sulphonyl ureas, acetoanilides, benzimidazoles, pyrethroids, diphenyl ethers and the recently introduced imidazolinones [2, 13-19].

2.3.1. Need for Pesticides Analysis

Environmental pollution has been known as a world-wide problem for many years, and pesticides are one of its primary causes.

Pesticide use has been increasing in household, in agriculture and other areas. It is recognized that pesticides are harmful to human beings, but it should also be remembered pesticides are chemical substances that are essential to maintain a high quality of life for human beings.

Residual pesticides in foods, drinks and the environment have been analysed in the fields of environmental chemistry, forensic chemistry, and preventive medicine. So the need for pesticide analysis is well established.

2.3.2. Organophosphorous pesticides

Organophosphorous pesticides (OPPs) were introduced to the market in the period 1945-55 to replace the toxic and persistent organochlorine insecticides, mainly DDT. They represent the family of about 140 different compounds, which are classified in different groups depending on their chemical structure. They are esters, amides or thiols which in general derive from phosphoric or phosphonic acid, where one or more atoms of hydrogen are substituted by organic groups. Depending on functional groups, OPPs are divided into six groups or families: phosphates, phosphonates, phosphorothioates, phosphorodithioates, phosphorothiolates and phosphoroamidates. Because P=S bond is the most stable, many OPPs are synthesized with such a configuration. The characteristics of each group of OPPs can vary substantially, and they confer the specificity to react against one type of organism or another. In general terms, the mode of action of OPPs is based on the inhibition of the enzyme acetylcholine esterase of the organism, which blocks the nervous transmission and produces death normally by respiratory depression. Owing to this specificity and because they are rapidly degraded after application and rarely accumulated in the trophic chain, OPPs are extensively used to combat different pests. The main uses are in agricultural crop production, industrial activities and in the tertiary sector (domestic use, mosquito and rodent control, greenhouses, cemeteries, aquaculture etc). In such practices, OPPs are applied as formulations to enhance their effectiveness upon application, absorption, translocation, immobilization and detoxification. Formulations contain additives and adjuvants such as mixtures of surfactants, minerals and vegetable oils, emulsifiers and salts.

Methyl Parathion is one of the most widely applied organophosphorous insecticide in agriculture. This insecticide is widely used to control chewing and sucking insects in a wide range of crops [3]. Because of the high toxicity, methyl parathion is not approved for non-professional use. Poisoning with methyl parathion lead to cholinergic overstimulation, with signs of toxicity including seating, dizziness, vomiting, diarrhea, convulsions, cardiac arrest, respiratory arrest, and, in extreme cases, death.

Methyl parathion enters the environment primarily by spraying on farm crops, but it breaks down quickly to other chemicals such as methyl paraoxon, p-nitro phenol, dimethyl phosphoric acid, methyl phosphorothioic acid and amino methyl parathion as a consequence of biodegradation, hydrolysis, interactions with natural organic matter and photolysis [2].

3. Literature Review

The environmental pollution capacity of MPT, or as general OPPs, has been the concern of many scientists. Many studies have been conducted in different fields that emphasize on the effects, concentration level, distribution, use and other points of the pesticides [3, 20-32].

Electrochemical methods are also widely used for the detection and determination of MPT. Development of reliable and sensitive procedure is mandatory to draw a better conclusion. In this regard, different scholars developed different electrochemical procedures.

J. Kumar et al. developed an optical microbial biosensor for the detection of MPT pesticide using *Flavobacterium SP.* whole cells adsorbed on glass fiber filters as disposable biocomponent. The detection of MPT was simple, single step and direct measurement of very low quality of the sample. A lower detection limit 0.3 μ M MPT is estimated from linear range (4-80 μ M) of calibration plot of organophosphorous hydrolase enzymatic assay [20].

J. Gong et al. developed a simple strategy for designing a highly sensitive electrochemical biosensor for OPPs based on acetylcholinesterase immobilized onto Au nanoparticles-polypyrrole nanowires composite film modified glassy carbon electrode [21]. The combination of Au nanoparticles and polypyrrole nanowires greatly catalyzed the oxidation of the enzymatically generated thiocholine product, thus increasing the detection sensitivity.

A sensitive voltammetric procedure for the determination of MPT at a glassy carbon electrode modified with a single-walled carbon nano-tube /dicetyl phosphate composite film has been developed by Chunya Li et al. Under optimized conditions, a linear response between the

reduction peak current and the methyl parathion concentration is obtained from 5.0×10^{-7} to 1.0×10^{-4} M with a detection limit of 2.0×10^{-7} M [22].

Shuangshuang Fan et al. developed an ionic liquid (i.e. 1-butyl-3-methylimidazolium hexafluorophosphate, BMIMPF₆) – single-walled carbon nanotube (SWNT) paste coated glassy carbon electrode [24]. The electrode shows a good electro-catalysis to the reduction of MPT. Under optimized conditions the peak current is linear to MPT concentration over the range of 2.0×10^{-9} M to 4.0×10^{-6} M. The detection limit is 1.0×10^{-9} M. In addition, hydrolysate of MPT (i.e. p-nitrophenol) can also produce a sensitive cathodic peak under the same condition and can be determined simultaneously with MPT.

G. M. Castanho et al. used a differential pulse polarography technique to establish an electroanalytical procedure for the determination of MPT in soil samples. The limit of detection was 1.93×10^{-8} M for pure water and about 8×10^{-8} M for soil suspensions with a scan rate of 2mV/sec and a pH of 6.75 [25].

Mohammed Sbai et al. developed a novel carbon fiber microelectrode obtained by tetrasulfonated phthalocyanine electrodeposition on carbon surface combined with Nafion[®] coating for the detection of Methyl Parathion (MPT) [36].

A fast and ultra-sensitive trace analysis of Methyl Parathion pesticides in a dimethylsiloxane (PDMS) microfluidic channel was investigated by Donghoon Lee et al. using confocal surface-enhanced Raman spectroscopy (SERS) [37].

4. Objective of the Study

Many conducting polymers are used to develop a sensitive electrochemical method for different analytes' detection and the results found are encouraging.

Different electrochemical methods have been applied for the study of MPT (or OPPs). These methods have their own qualities and drawbacks. Continual search for a better sensor is needed for better judgments. So, this study was conducted with the following objectives:

- 1) To develop a sensitive electrochemical procedure for MPT detection.
- 2) To use a conducting polymer for a sensitive detection of MPT.

5. Experimental

5.1.Apparatus

Voltammetric measurements were performed using BASi CV-50W Electrochemical Analyser connected to a personal computer. A three electrode configuration was employed, Consisting of a polymer (poly-AHNSA) modified glassy carbon electrode(d=3mm), Ag/AgCl/KCl(3M), and a platinumium wire as the working, reference and counter electrode, respectively.

All experiments were performed at room temperature.

5.2. Reagents

Methyl Parathion (MPT), 4-Amino-3-Hydroxynaphthalene-1-Sulphonic acid (AHNSA) dissolved in 0.1M HNO₃, Acetate buffer (pH 3 – pH 6) , Phosphate buffer (pH 7) , 0.5M H₂SO₄ .

All the solutions were prepared using distilled water as a solvent unless otherwise stated.

5.3. Procedures

5.3.1. Preparation of Poly-AHNSA/GCE

A 2 mM AHNSA (monomer) solution made in 0.1M HNO₃ was made to electropolymerize on a 3mm diameter glassy carbon electrode using cyclic Voltammetry between switching potentials of -800mV and 2000mV for 25 cycles.

After completing the 25 cycled electropolymerization, the modified electrode was made to stabilize employing cyclic Voltammetry with switching potentials -800mV and 800mV in pH 5 acetate buffer for 3 x 16 cycles.

5.3.2. Measurement Procedures

First electrochemical behavior of Methyl Parathion was examined by cyclic Voltammetry using the modified electrode.

Then a suitable voltammetric technique which gives a better peak current was chosen. Next, optimizations of accumulation potential, accumulation time and solution pH were employed using square wave Voltammetry scanned from potential of -300mV to -800mV.

With the same potential window analytical characterization of MPT solution having different concentrations was employed.

6. Result and Discussion

6.1. Electropolymerization of AHNSA

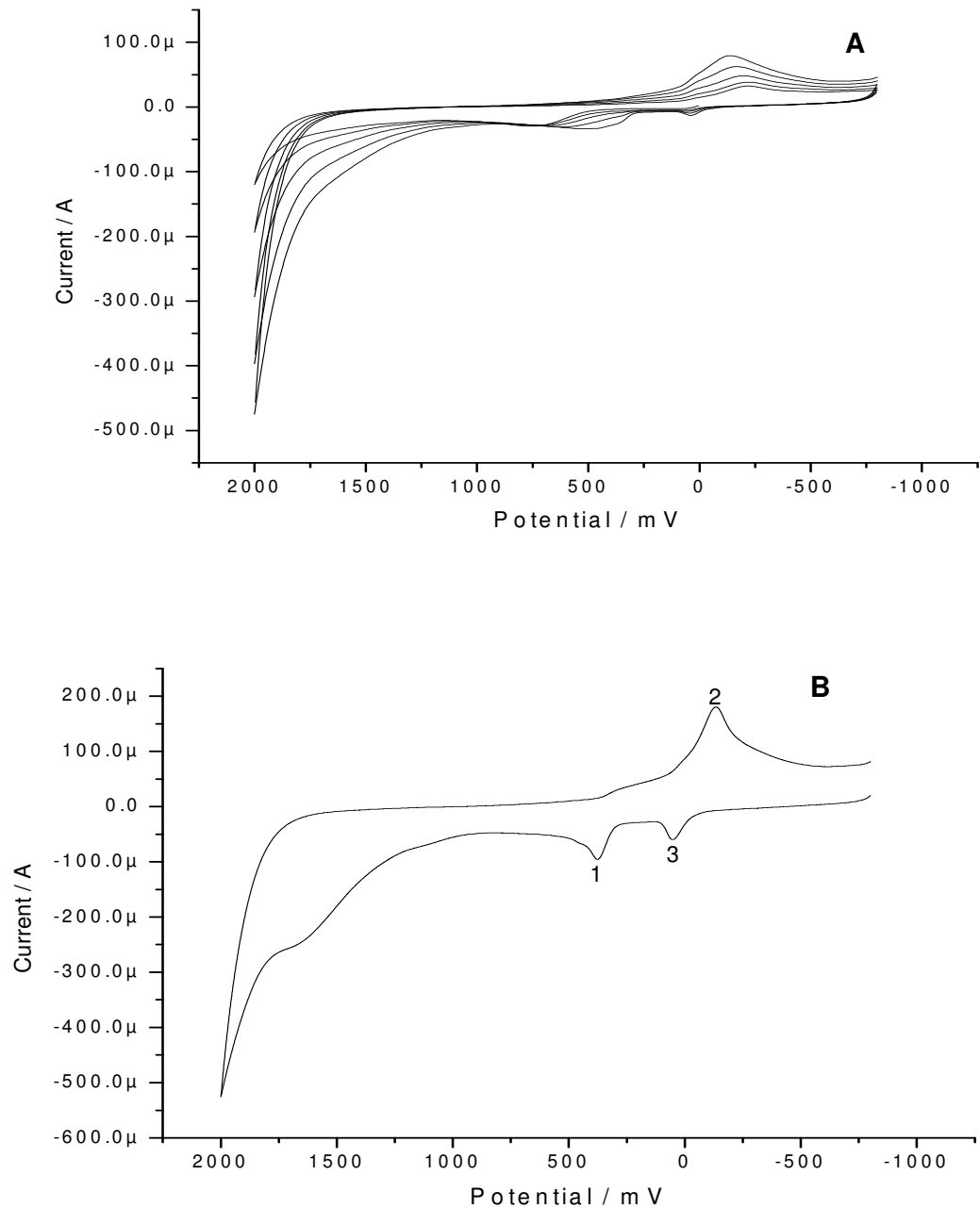


Fig. 13. (A) continuous cyclic voltammogram of AHNSA in 0.1M HNO₃; (B) the 26th cyclic voltammogram of AHNSA in 0.1MHNO₃; scan rate: 100mV/s, switching potentials: +2000mV and -800mV.

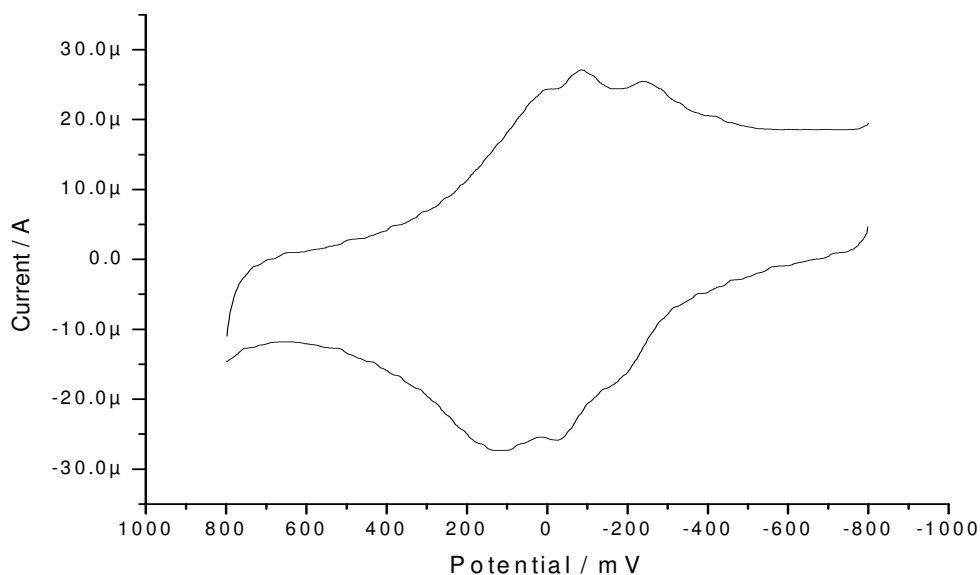
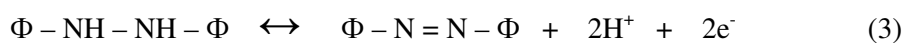
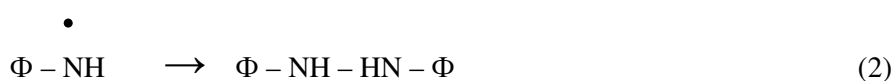
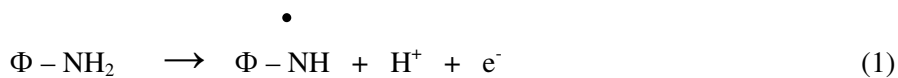
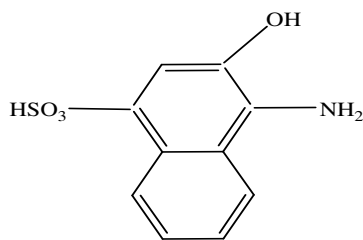


Fig. 14. cyclic voltammogram at poly-AHNSA/GCE modified electrode in pH 5 acetate buffer solution; scan rate: 100mV/s, switching potentials: +800mV and -800mV.

The proposed mechanism for the above voltammogram looks like: [33]



Where $\Phi - \text{NH}_2$ is



4-Amino-3-Hydroxynaphthalene-1-Sulphonic acid (AHNSA)

It is shown in fig. 13. A and B that peak 1 is first formed which corresponds to the formation of a radical (eq. 1). Because this radical is unstable, it combines with other radical to form Hydrazohydroxynaphthalene sulphonic acid that gave peak 2 (eq. 2). Peak 3 appears slowly. This is because the product from eq. 2 is relatively stable that it took certain time to reach at equilibrium forming Azohydroxynaphthalene sulphonic acid (eq. 3).

Fig.14. shows a 1 cycle cyclic voltammogram of monomer free poly-AHNSA. This voltammogram was taken just before the modified electrode is used for MPT detection. It can be seen that peaks formed during MPT detection (fig . 16) are not due to the polymer on the surface of the glassy carbon electrode.

6.2. Electrochemical Behavior of Methyl Parathion

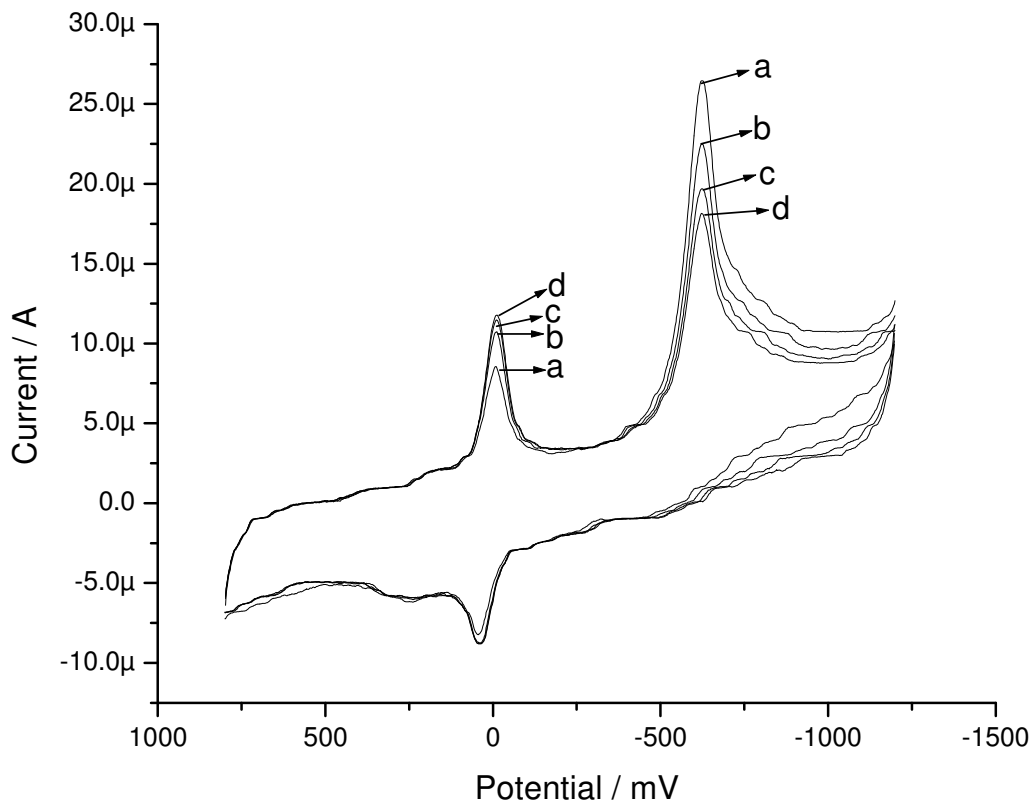
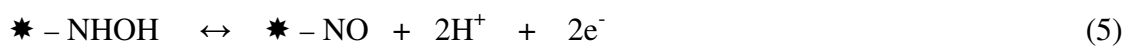


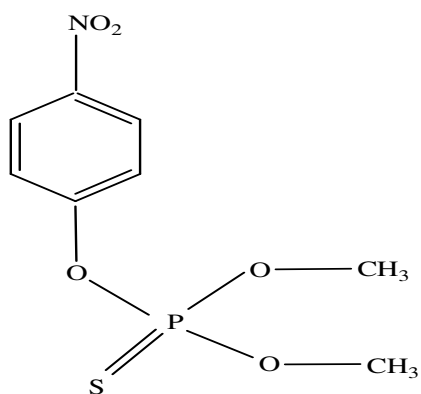
Fig. 15. Continuous CV response of $8\mu\text{M}$ MPT at the poly-AHNSA modified GCE in pH5 acetate buffer. Scan rate: 100mV/s ; switching potentials: $+800\text{mV}$ and -1200mV .

In the first cathodic scan of fig. 15. , an intense peak at a potential of about 600 mV is observed. Then other peaks appeared at a potential of 42mV during the first anodic scan and at a potential of -9mV during the second cathodic scan with both having a smaller peak current. However, during successive scans, the two peaks at a potential of -9 mV and 42mV increase with the expense of the peak appeared at 600mV. This clearly indicates that MPT is first irreversibly reduced and the reduced form is further reduced to form a reversible products.

The mechanism suggested in different literatures looks like [34, 35]



Where * - NO₂ is



Methyl Parathion (MPT)

6.3. Effect of poly-AHNSA on MPT Detection

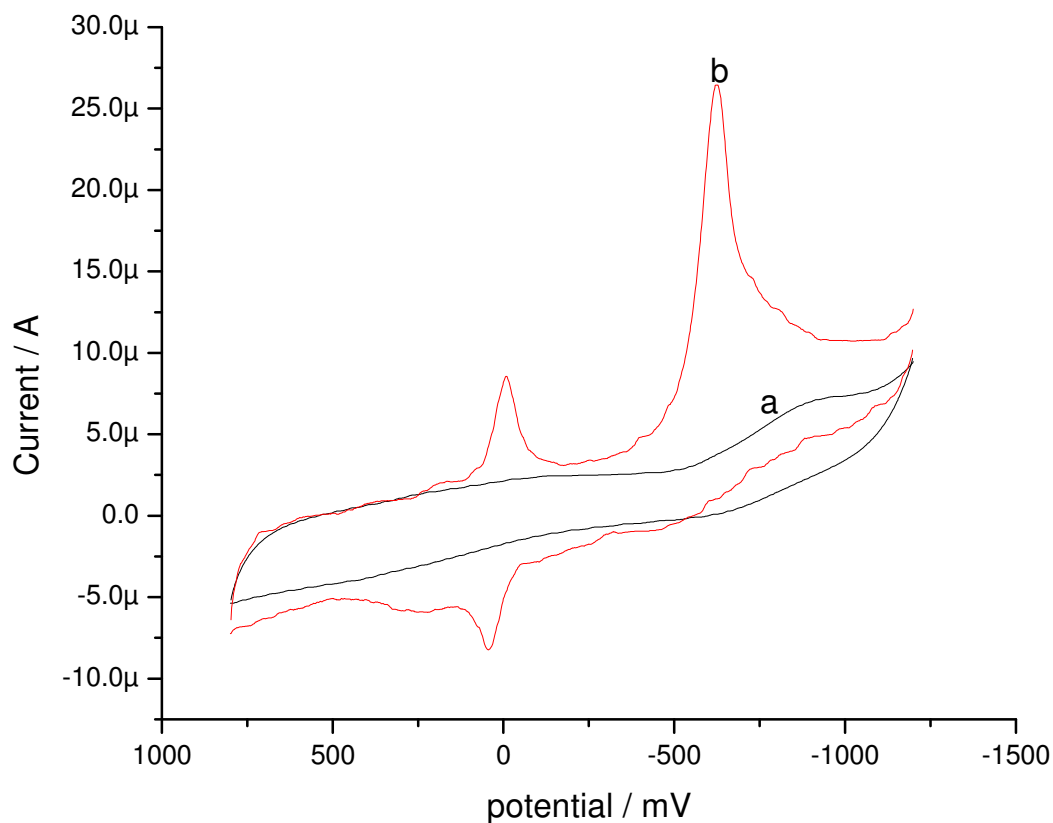


Fig. 16. Cyclic voltammograms of 8 μ M MPT at bare GCE (a) and poly-AHNSA/GCE. Scan rate: 100mV/s; switching potentials: +800mV and -1200mV.

As it can be seen from fig. 16, both the cyclic voltammogram in the presence (at the polymer modified GCE) and absence (at the bare GCE) of poly-AHNSA, the presence of MPT in the solution is well detected using the former electrode. The bare can barely detect MPT in the solution even using square wave Voltammetry. But with polymer modified GCE, the three peaks we expect from MPT are visibly detected. This shows the presence of poly-AHNSA made a difference on the detection of MPT.

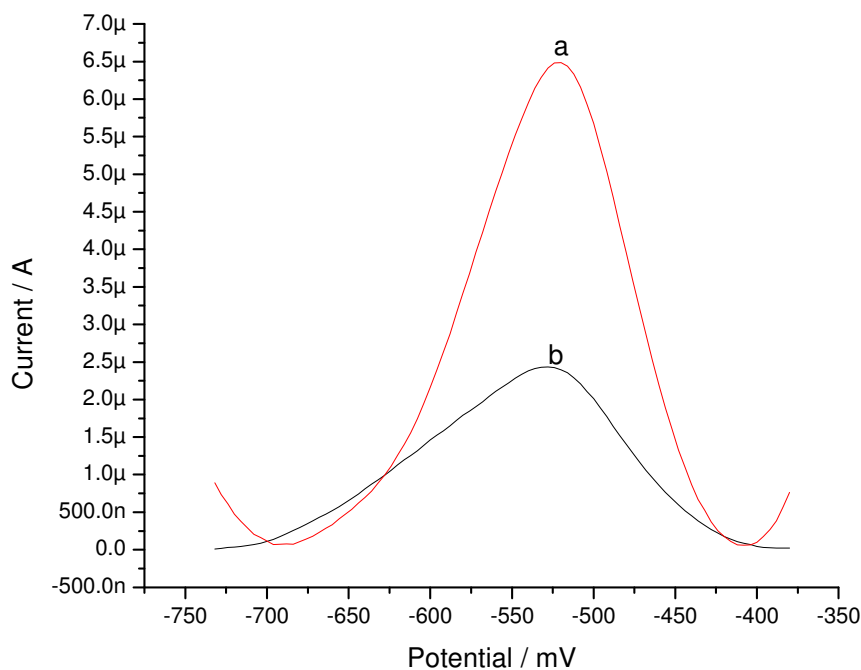


Fig. 17. Square wave (a), differential pulse (b) voltammetric response of 10 μ M MPT at the poly-AHNSA/GCE in pH acetate buffer. Scan rate: 100mV/s; $P_p = -0.4V$; $t_p = 50$ s.

Selection of voltammetric technique was also made. As it can be seen in fig. 17 square wave Voltammetry gave the highest peak current response for the same concentration of MPT. So, square wave Voltammetry is choose for the process.

6.4. Optimization of Parameters for MPT Detection

For better and enhanced peak current response, selection of parameters (conditions) is vital. In this project optimization of accumulation potential, accumulation time and solution pH are conducted for the final detection of MPT.

6.4.1. Effect of Accumulation Potential (P_p)

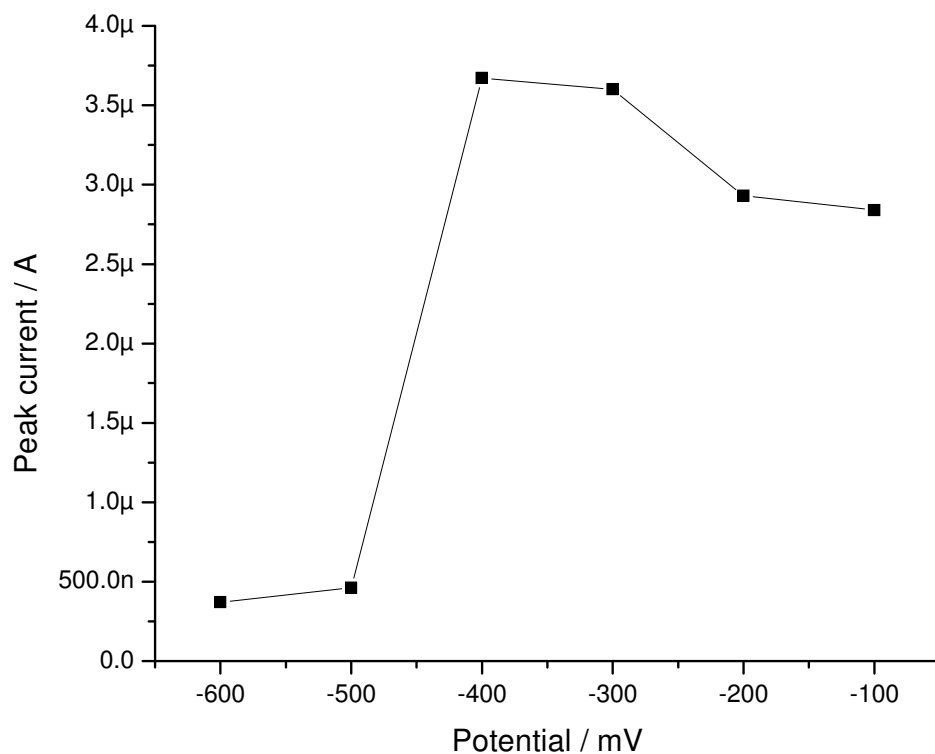


Fig. 18. Effect of P_p on square wave voltammetric response for $8\mu\text{M}$ MPT in pH 5 acetate buffer at poly-AHNSA/GCE. $t_p = 50$ s; SW amplitude: 25mV ; frequency: 15mV ; step : 4mV .

Selection of the optimum potential is necessary for a maximum deposition of our analyte in the form of the species that gives response at a potential of 600mV (on CV) on the polymer modified GCE. Fig. 18 shows that an accumulation potential of -400mV gives the maximum peak current. This is consistent with the fact that a potential closer but more positive to the reduction potential of the species will not affect the nature of the species but it makes it more abundant at the surface of the electrode.

More negative potentials like -500mV, -600mV etc essentially tend to reduce the species and convert it into its other forms which, already mentioned, give peaks at another potentials.

6.4.2. Effect of Accumulation Time (t_p)

The main goal of searching different analytical methods is to find an analytically valuable data with considerably shorter time. So, in this context, the accumulation process which gives a good peak current response with a shorter time is advantageous.

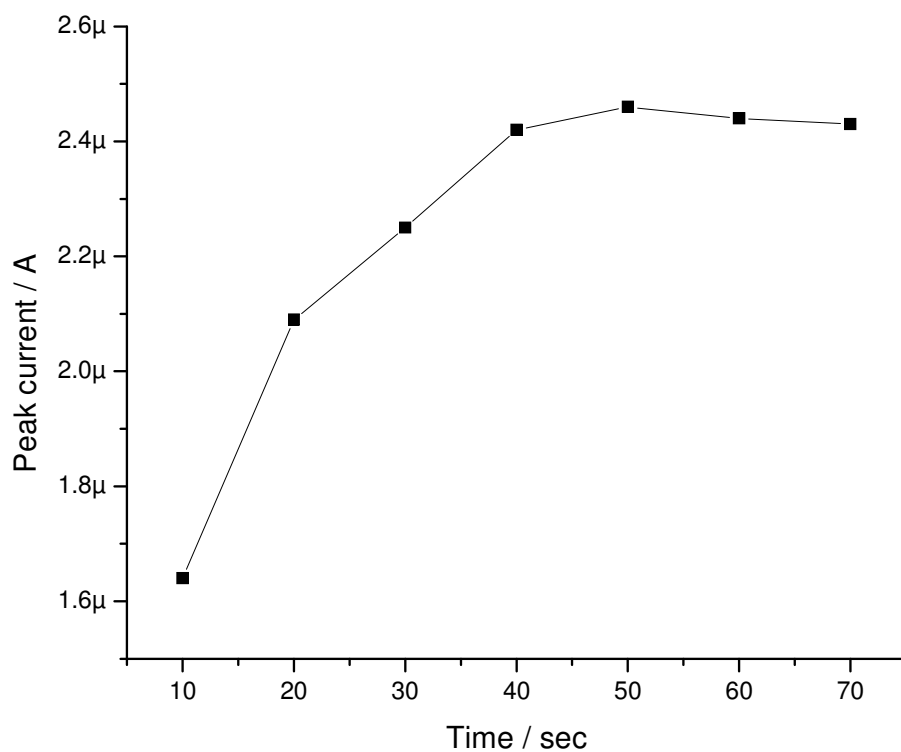


Fig. 19. Effect of t_p on square wave voltammetric response for 8 μM MPT in pH 5 acetate buffer at poly-AHNSA/GCE. $P_p = -0.4$ s; SW amplitude: 25mV; frequency: 15mV; step : 4mV.

Fig. 19 shows that the current response increases rapidly till a 40 sec accumulation time and still increases at a 50 sec accumulation time. This accumulation time gives a good current response and chosen for the process.

6.4.3. Effect of Solution pH

In eq. 4 and 5, it is been shown that the reduction of MPT is pH dependent. This makes choosing an appropriate solution pH vital for the analysis.

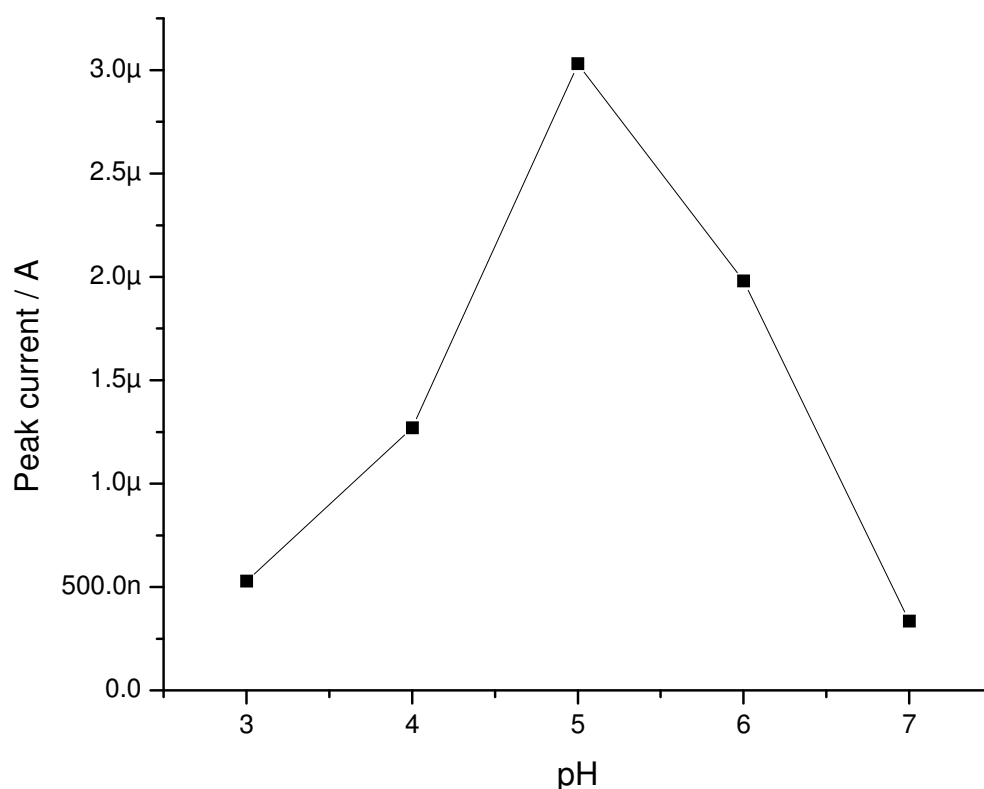


Fig. 20. pH dependence of peak current on SW voltammetric response for 8μM MPT at the poly-AHNSA/GCE. $P_p = -0.4V$; $t_p = 50$ s; SW amplitude:25mV; frequency: 15mV; step : 4mV.

Fig. 20 shows a plot of peak current Vs pH. The maximum peak current is found from the solution with pH 5. Therefore pH 5 is taken as an appropriate pH for the analysis.

Generally, for the analysis of MPT using polymer modified GCE an accumulation potential of -400mV, accumulation time of 50 sec and a pH 5 solution are been chosen.

6.5. Analytical characterization

Fig. 21 shows square wave voltammograms of MPT at bare and poly-AHNSA/GCE with increasing concentration of MPT from 0.2 μ M to 1.6 μ M. As expected the current response tend to increase with increase in concentration.

Fig. 22 shows the calibration curve of the poly-AHNSA/GCE for the determination of Methyl parathion.

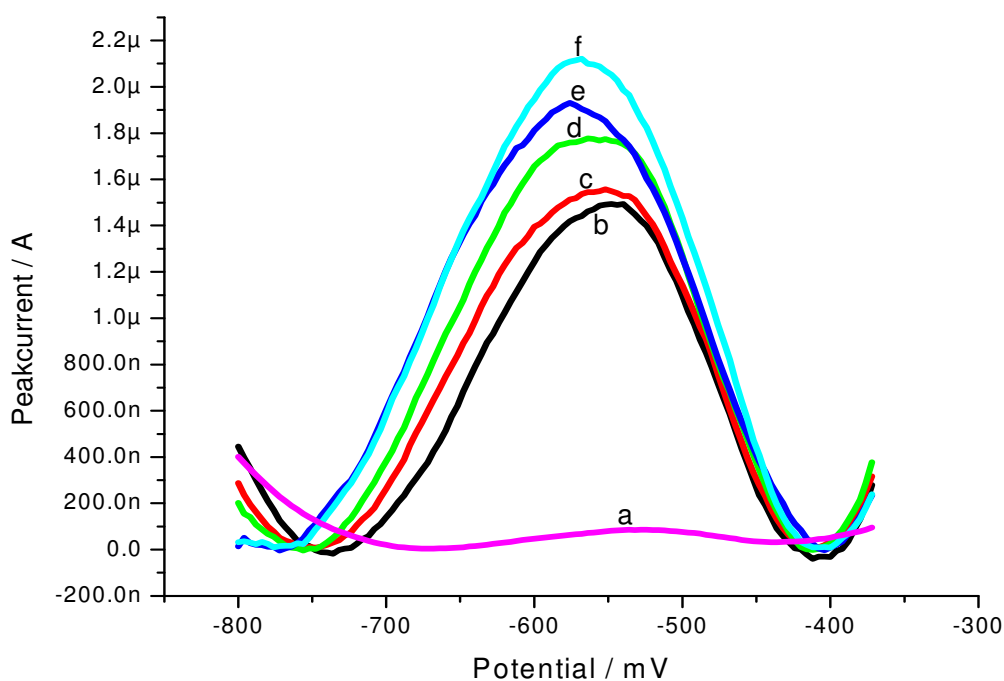


Fig. 21. Square wave voltammograms of increasing concentration of MPT at poly-AHNSA/GCE in pH 5 acetate buffer. (a) blank solution; (b) 0.2×10^{-6} M; (c) 0.4×10^{-6} M; (d) 0.8×10^{-6} M; (e) 1.2×10^{-6} M; (f) 1.6×10^{-6} M. $P_p = -0.4$ V; $t_p = 50$ s; SW amplitude:25mV; frequency: 15mV; step : 4mV.

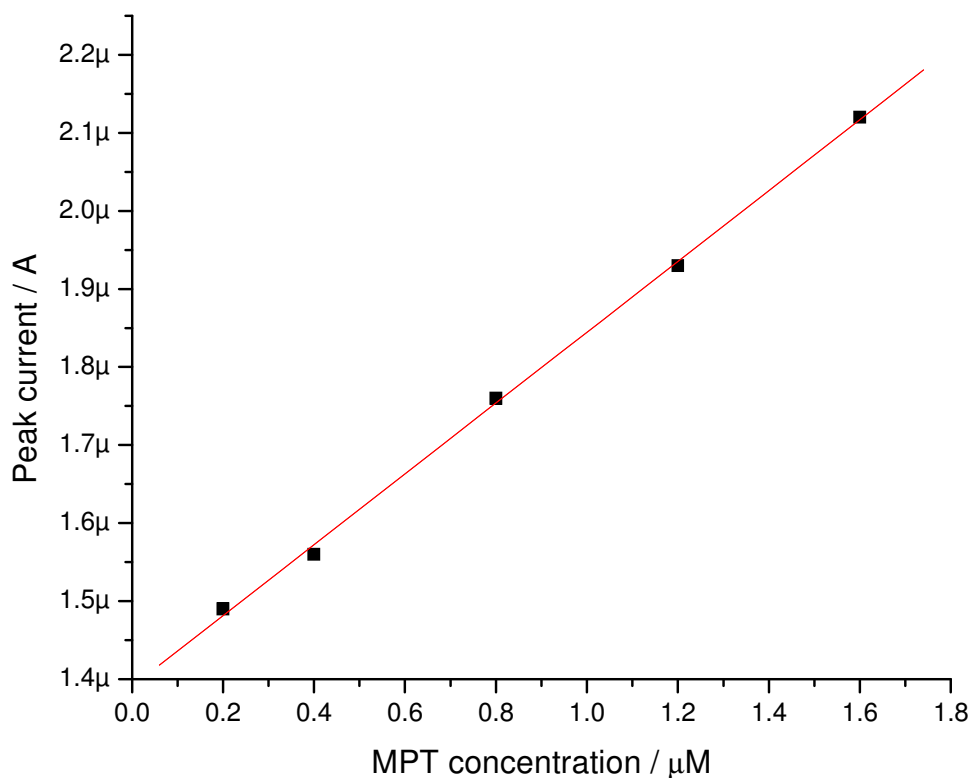


Fig. 22. A plot of peak current Vs MPT concentration. $P_p = -0.4\text{V}$; $t_p = 50 \text{ s}$; SW amplitude:25mV; frequency: 15mV; step : 4mV.

Using the optimized conditions, the modified electrode exhibits a linear relationship between the peak current and the concentration of MPT. The linearity has a correlation coefficient of 0.999. This shows a good linear response for increase in concentration. The detection limit was $6.3 \times 10^{-8}\text{M}$ calculated using a measured value of blank solution with poly-AHNSA/GCE.

7. Conclusion

Electrodes are being modified with polymers seeking a better sensor than those already are in effect.

With this project a GCE is been modified with poly-AHNSA for the detection of MPT. The results found suggest that the modified GCE gave a good response for MPT with a linear increase in peak current with increase in concentration. It has a correlation coefficient of 0.999 and detection limit of $6.3 \times 10^{-8} \text{M}$.

The following table compares the detection limit obtained in this project with that some other detection limits found previously using other electrode modification procedures.

Table 1. Comparison of detection limits for procedures with different modified electrodes

Sensor	Analyte	Detection limit
a	MPT	$3 \times 10^{-7} \text{M}$
b	MPT	$2 \times 10^{-7} \text{M}$
c	MPT	$1 \times 10^{-9} \text{M}$
d	MPT	$1.93 \times 10^{-8} \text{M}$
e	MPT	$6.3 \times 10^{-8} \text{M}$

a = optical biosensor using *Flavabacterium SP*. Whole cells adsorbed on glass fiber filters^[20]

b = GCE modified with a single-walled carbon nano-tube /dicetyl phosphate composite film^[22]

c = an ionic liquid (i.e. 1-butyl-3-methylimidazolium hexafluorophosphate, BMIMPF₆) – single-walled carbon nanotube (SWNT) paste coated glassy carbon electrode^[24]

d = mercury electrode^[25]

e = GCE modified with poly-(4-Amino-3-Hydroxynaphthalene-1-Sulphonic acid)

From the above table, the detection limit found in this project (e) is comparable with other procedures' detection limit.

So, it can be concluded that poly-AHNSA/GCE has a good detection limit and can be used for the detection of MPT.

Reference

1. Gerard, M., Chaubey, A., Malhotra, B. D. *Biosensors and Bioelectronics* **2002**, 17, 345-359
2. Lacorte, S., Barcelo, D. “Organophosphorous Pesticides in Water and Food Analysis”,
Encyclopedia of Analytical Chemistry, Meyers, R. A. Volume 7, Wiley, **2000**
3. Diagne, M., Oturan, N., Oturan, M. A. *Chemosphere* **2007**, 66, 841–848
4. Anderson T., Roth S. *Brazilian Journal of Physics* **1994**, 24, No.3, 746-754
5. Bredas, J. L., Street, G. B. *Acc. Chem. Res.* **1985**, 18, 309-315
6. Roth, S., Bleier, H., Pukacki, W. *Faraday Discuss. Chem. Soc.* **1989**, 88, 223-233
7. Skoog, D. A., West, D. M., Holler, F. J. *Fundamentals of Analytical Chemistry*, 7th ed.
Harcourt College Publishers **1997**, USA
8. Bard, J., Faulkner, L. R. *Electrochemical methods*, 2nd ed., Wiley, New York, USA, **2000**
9. J. Wang, *Analytical Electrochemistry*, 2nd ed., Wiley, New York, USA, **2001**
10. Skoog, D. A., Leary, J. J. *Principles of Instrumental Analysis*, 4th ed., Saunders College
publishing, USA
11. Protti, P. *Introduction to Modern Voltammetric and Polarographic Analysis Techniques*,
Amel Electrochemistry, 4th ed., New York , USA, **2001**
12. Lacourse, W. R. *Pulsed Electrochemical Detection in HPLC*, Wiley, New York, USA **1997**
13. Garrido, E. M., C., Matos, C. D., Lima, J. L. F., and A. M. O. Brett, A. M. O. *Analytical
letters* **2004**, 37, 1755-1791
14. Zakaria, Z., Heng L. Y. , Abdullah, P., Osman, R., Din, L. *Malaysian Journal of Chemistry*
2003, 8, 78-85

15. Hodgson, E. A Text Book of Modern Toxicology, 3rd ed., WILEY, New York, USA, **2004**
16. Manahan, S. E. Environmental Chemistry, 8th ed, , CRS press, **2005**
17. Blake, B. “ Toxicology of the Nervous System”, A Text Book of Modern Toxicology,
Hodgson, E. 3rd ed., Wiley, New York, USA, **2004**
18. Mavrikou, S. Flampouri, K., Moschopoulou, G., Mangana, O., Michaelides, A., Kintzios, S.
Sensors **2008**, 8, 2818-2832
19. Okumura, T., Imamura, K., Nishikawa, Y. *Analyst* **1995**, 120, 2675-2681
20. Kumar, J., Jha, S. K., D’Souza, S. F. *Biosensors and Bioelectronics* **2006**, 21, 2100–2105
21. Gong, J., Wang, L., Zhang, L., *Biosensors and Bioelectronics* **2009**, 24, 2285-2288
22. Li, C., Mo, W., Zhan, G., Sun, X. *Chem. Anal. (Warsaw)*, **2008**, 53, 201
23. Luciana B.O. Dos Santos, L. B. O., Masini, J. C. *analytica chimica acta* **2008**, 606, 209-216
24. Fan, S., Xiao, F., Liu, L., Zhao, F., Zeng, B. *Sensors and Actuators* **2008**, 132, 34-39
25. Castanho, G. M., Vaza, C. M. P., Sérgio A. S. Machado, S. A. S. *J. Braz. Chem. Soc.* **2003**,
14, 594-600
26. Muttraya, A., Spelmeyera, U., Degirmencia, M., Junga, D., Backerc, G., Hill, G.
Environmental Toxicology and Pharmacology **2005**, 19, 477–483
27. Zhou, X., Scharf, M. E., Sarath, G., Meinke, L. J. Chandler, L. D., Siegfried, B. D. *Pesticide
Biochemistry and Physiology* **2004**, 78, 114–125
28. Celik, I., Isik, I. *Pesticide Biochemistry and Physiology* **2009**, 94, 1–4
29. Krishna, K. R., Philip, L. *Journal of Hazardous Materials* **2008**, 160, 559–567

30. Piña-Guzmán, P., B., et al., Methyl-parathion decreases sperm function and fertilization capacity after targeting spermatocytes and maturing spermatozoa, *Toxicol. Appl. Pharmacol.* **2009**, doi:10.1016/j.taap.2009.05.008
31. Maitra, S. K., Mitra, A. *Ecotoxicology and Environmental Safety* **2008**, 71, 236–244
32. Celik, I., Suzek, H. *Journal of Hazardous Materials* **2008**, 153, 1117–1121
33. Jin, G., Zhang, Y., Cheng, W. *Sensors and Actuators B* **2005**, 107, 528-534
34. Liu, X., Li, C., Hu, S. *Microchimica Acta* **2006**, 154, 275-280
35. Zen, J., Jou, J., Kumar, A. S. *Analytica Chimica Acta* **1999**, 396, 39-44
36. Sbai, M., Essis-Tome, H., Gombert, U., Breton, T., Pontie, M. *Sensors and Actuators B* **2007**, 124, 368-375
37. Lee, D., Lee, S., Seong, G. H., Choo, J., Lee, E. K., Gweon, D., Lee, S. *Applied Spectroscopy* **2006**, 60, 373-377